

Supporting information for

Synthesis of fluorescent MOFs: live-cell imaging and sensing studies of herbicide

Aurobinda Mohanty^a, Udai P. Singh^{a*}, R. J. Butcher^b, Neeladrisingha Das^c, Partha Roy^c,

^aDepartment of Chemistry and ^cDepartment of Biotechnology, Indian Institute of Technology Roorkee, Roorkee – 247667, India.

E-mail: udaipfcy@iitr.ac.in; Tel: +91-1332-285329

^bDepartment of Chemistry, Howard University, Washington, DC 20059, USA.

GENERAL METHODS

Sample Characterization

¹H NMR and ¹³C NMR spectra were recorded using a Bruker-400 spectrometer with tetramethylsilane as the internal standard. HRMS were recorded on a Bruker microTOF-Q-II mass spectrometer (ESI-MS). Powder diffraction XRD investigations were carried out on a Bruker D8 diffractometer (CuK α , $\lambda = 1.540 \text{ \AA}$) at 296 K. Fluorescence spectra were recorded on a RF-5301PC spectro-fluorophotometer (Shimadzu) with the excitation wavelength of 315 nm and the slit width 2.0 nm for both the excitation and emission. The fluorescence decay profiles were recorded by exciting the sample at 315 nm using a Horiba Jobin Yvon “fluorocube FL” life time system equipped with new LED (635 nm) source. UV–vis spectra were measured on an Agilent Cary 100 spectrophotometer using a pair of quartz cells (3.5 mL volume) of 10 mm path length. Thermal analyses (TGA) were performed at a heating rate of 10 °C/min from 20 to 600 °C using Perkin-Elmer Pyris Diamond DSC and Pyris Diamond thermogravimetry analyzers, respectively.

Crystallography Details

A suitable crystal was mounted on a loop and the X-ray data of all the MOFs were collected on a Bruker Kappa Apex four circle-CCD diffractometer using graphite monochromated MoK α radiation ($\lambda = 0.71070 \text{ \AA}$) at 296 K. Crystal structures were solved by direct methods¹. Structure solutions, refinement and data output were carried out with the SHELXTL program². Thermal parameters for all non-hydrogen atoms were refined anisotropically. Images and hydrogen bonding interactions were created in the crystal lattice with DIAMOND³ and MERCURY.⁴ Topological analysis was performed by using the program “TOPOS-4.0.”⁵ The marginally high R indices are due to the presence of thermal disorder of solvent in addition to the poor quality of data. The SQUEEZE tool of PLATON was applied to 1, 3, 4 and 7 for the existence of large solvent-accessible voids. The crystallographic data

are summarized in Table S1. Selected bond lengths and angles are given in Tables S2. The Crystallographic data (excluding structure factors) for the structures reported in this paper have been deposited with the Cambridge Crystallographic Data Centre (CCDC) as deposition Nos. CCDC1976414-1976421

Table S1. Crystal data and Collection Details of MOFs1-8.

	MOF1	MOF2	MOF3	MOF4	MOF5	MOF6	MOF7	MOF8
CCDC	1976414	1976415	1976416	1976417	1976418	1976419	1976420	1976421
Empirical formula	C ₃₉ H ₃₅ N ₃ O ₉ S ₂ Zn	C ₄₁ H ₄₄ N ₄ O ₉ S Zn	C ₃₃ H ₂₃ N ₂ O ₇ S Zn	C ₆₈ H ₆₀ Cd N ₆ O ₁₂ S ₂	C ₃₆ H ₂₆ Cd N ₂ O ₈ S ₂	C ₄₂ H ₄₄ Cd N ₄ O ₁₂ S ₂	C ₁₃₆ H ₁₀₃ Cd ₄ N ₈ O ₄₀ S ₄	C ₇₈ H ₇₇ Cd ₂ N ₈ O ₂₂ S ₂
Formula weight	817.19	834.25	656.98	1329.74	791.12	973.33	3067.15	1767.42
Crystal System	Triclinic	Monoclinic	Monoclinic	Triclinic	Triclinic	Triclinic	Monoclinic	Triclinic
Space Group	P -1	P 21/n	P 21/c	P -1	P -1	P -1	P 21/m	P -1
Temp. (K)	296(2) K	296(2)K	296(2)K	296(2) K	296(2) K	296(2)K	296(2) K	296(2) K
<i>a</i> / Å	11.0983(6)	10.3347(15)	14.7151(8)	10.1650(6)	11.485(3)	7.2438(12)	19.0496(5)	10.4780(3)
<i>b</i> / Å	13.4007(7)	28.128(4)	16.6827(8)	12.5470(7)	14.804(4)	12.0019(14)	19.2025(6)	10.9252(4)
<i>c</i> / Å	14.5973(8)	13.679(2)	15.1237(8)	14.9573(8)	15.054(6)	12.4874(13)	26.8670(8)	18.8828(6)
<i>α</i> / °	76.060(3)	90	90	69.583(2)	115.689(17)	106.752(10)	90	74.757(1)
<i>β</i> / °	73.461(3)	103.218(10)	111.547(3)	89.940(2)	110.529(17)	96.043(11)	90.030(2)	85.243(2)
<i>γ</i> / °	83.396(3)	90	90	81.668(2)	95.410(12)	101.010(12)	90	66.579(1)
<i>V</i> / Å ³	2017.35	3871.1(10)	3453.21	1766.42(17)	2066.0(13)	1005.5(2)	9828.0(5)	1913.15
<i>Z</i>	2	4	4	1	2	1	2	1
<i>D</i> _{calc} / g cm ⁻³	1.345	1.428	1.264	1.250	1.272	1.607	1.036	1.534
F(000)	844.0	1738.36	1348.0	686.0	800.0	500.0	3102.0	905.0
<i>μ</i> / mm ⁻¹	0.768	0.750	0.817	0.429	0.675	0.718	0.528	0.692
<i>θ</i> range / °	1.491 to 28.364°.	3.122 to 28.495°.	2.727 to 28.424°.	1.455 to 28.296°.	1.596 to 28.628°.	2.907 to 35.117°.	0.758 to 28.358°.	1.118 to 28.282°.
Reflections collected	35665	46735	46045	30173	33668	14977	114040	32457
Independent reflections	10008	9597	8587	8680	10250	14977	25097	15763
Complete to 2 θ	99.6	98.8	99.8	99.5	99.8	98.0	99.5	99.5
Data / restraints / parameters	10008 / 6 / 496	9597 / 0 / 514	8587 / 0 / 398	8680 / 150 / 454	10250 / 3 / 470	14977 / 15 / 291	25097 / 0 / 896	15763 / 3 / 1022
GOF (<i>F</i> ²)	1.021	0.965	0.986	1.027	1.097	1.158	0.914	1.036
<i>R</i> 1; <i>wR</i> 2 [<i>I</i> > 2 σ (<i>I</i>)]	<i>R</i> 1 = 0.0625, <i>wR</i> 2 = 0.1998	<i>R</i> 1 = 0.0677, <i>wR</i> 2 = 0.1609	<i>R</i> 1 = 0.0583, <i>wR</i> 2 = 0.1661	<i>R</i> 1 = 0.0621, <i>wR</i> 2 = 0.1761	<i>R</i> 1 = 0.0761, <i>wR</i> 2 = 0.2172	<i>R</i> 1 = 0.1271, <i>wR</i> 2 = 0.3116	<i>R</i> 1 = 0.0731, <i>wR</i> 2 = 0.1872	<i>R</i> 1 = 0.0409, <i>wR</i> 2 = 0.1005
<i>R</i> 1; <i>wR</i> 2 (all data)	<i>R</i> 1 = 0.0940, <i>wR</i> 2 =	<i>R</i> 1 = 0.1949, <i>wR</i> 2 =	<i>R</i> 1 = 0.1026, <i>wR</i> 2 =	<i>R</i> 1 = 0.0621, <i>wR</i> 2 =	<i>R</i> 1 = 0.0995, <i>wR</i> 2 =	<i>R</i> 1 = 0.1326, <i>wR</i> 2 =	<i>R</i> 1 = 0.1702, <i>wR</i> 2 =	<i>R</i> 1 = 0.0548, <i>wR</i> 2 =

0.2242 0.1897 0.1926 = 0.1947 0.2554 0.3179 0.2329 0.1033

Table S2. Bond lengths [Å] and angles [°] for MOFs1-8

Bond angle and bond distance of MOF1

Zn(1)-O(5)	1.921(3)	Zn(1)-O(1)	1.939(3)
Zn(1)-O(6)	1.941(4)	Zn(1)-O(2)	1.940(2)
O(5)-Zn(1)-O(6)	105.29(18)	O(5)-Zn(1)-O(2)	101.82(11)
O(5)-Zn(1)-O(1)	109.85(12)	O(6)-Zn(1)-O(2)	122.80(15)
O(6)-Zn(1)-O(1)	107.8(2)	O(1)-Zn(1)-O(2)	108.66(12)
S(2)-O(2)-Zn(1)	134.51(15)	S(1)-O(6)-Zn(1)	133.0(3)
C(5)-O(1)-Zn(1)	131.1(3)	C(32)-O(5)-Zn(1)	128.7(2)

Bond angle and bond distance of MOF2

Zn(1)-O(1)	1.918(4)	Zn(1)-O(6)	1.988(4)
Zn(1)-O(7)	1.975(4)	Zn(1)-O(2)	2.080(5)
O(1)-Zn(1)-O(7)	109.50(15)	O(1)-Zn(1)-O(2)	104.6(2)
O(1)-Zn(1)-O(6)	134.79(18)	O(7)-Zn(1)-O(2)	93.75(17)
O(7)-Zn(1)-O(6)	106.10(16)	O(6)-Zn(1)-O(2)	99.86(19)
C(30)-O(6)-Zn(1)	102.7(3)	C(7)-O(7)-Zn(1)	127.1(3)
C(1)-O(1)-Zn(1)	131.0(4)	S(2)-O(2)-Zn(1)	128.9(3)

Bond angle and bond distance of MOF3

Zn(1)-O(2)	1.936(3)	Zn(1)-O(3)	1.955(3)
Zn(1)-O(1)	1.956(3)	Zn(1)-O(4)	1.986(3)
O(2)-Zn(1)-O(1)	100.41(12)	O(1)-Zn(1)-O(4)	102.35(13)
O(2)-Zn(1)-O(3)	124.36(14)	O(3)-Zn(1)-O(4)	110.37(12)
O(1)-Zn(1)-O(3)	99.94(12)	C(27)-O(3)-Zn(1)	108.3(3)
O(2)-Zn(1)-O(4)	114.80(15)	C(26)-O(2)-Zn(1)	140.0(3)
S(2)-O(4)-Zn(1)	134.66(17)	C(22)-O(1)-Zn(1)	141.9(3)

Bond angle and bond distance of MOF4

Cd-O(1S)#1	2.273(10)	Cd-O(1)#1	2.266(4)
Cd-O(1S)	2.273(10)	Cd-O(1)	2.266(4)
Cd-O(2)	2.249(4)	Cd-O(1T)	2.381(8)
Cd-O(2)#1	2.249(4)	Cd-O(1T)#1	2.381(8)

O(1S)#1-Cd-O(1S)	180.0	O(1S)-Cd-O(1)#1	92.2(5)
O(1S)#1-Cd-O(2)	93.2(4)	O(2)-Cd-O(1)#1	89.57(15)
O(1S)-Cd-O(2)	86.8(4)	O(2)#1-Cd-O(1)#1	90.43(15)
O(1S)#1-Cd-O(2)#1	86.8(4)	O(1S)#1-Cd-O(1)	92.2(5)
O(1S)-Cd-O(2)#1	93.2(4)	O(1S)-Cd-O(1)	87.8(5)
O(2)-Cd-O(2)#1	180.0	O(2)-Cd-O(1)	90.43(15)
O(1S)#1-Cd-O(1)#1	87.8(5)	O(2)#1-Cd-O(1)	89.57(15)
O(1)#1-Cd-O(1)	180.0	O(1S)-Cd-O(1T)#1	178.5(6)
O(2)-Cd-O(1T)	87.3(3)	O(2)-Cd-O(1T)#1	92.7(3)
O(2)#1-Cd-O(1T)	92.7(3)	O(2)#1-Cd-O(1T)#1	87.3(3)
O(1)#1-Cd-O(1T)	90.8(4)	O(1)#1-Cd-O(1T)#1	89.2(4)
O(1)-Cd-O(1T)	89.2(4)	O(1)-Cd-O(1T)#1	90.8(4)
O(1S)#1-Cd-O(1T)#1	1.5(6)		

Bond angle and bond distance of MOF5

Cd(1)-O(3)	1.937(5)	Cd(1)-O(6)	1.942(5)
Cd(1)-O(5)	1.939(5)	Cd(1)-O(4)	1.976(4)
O(3)-Cd(1)-O(5)	114.3(2)	O(5)-Cd(1)-O(4)	111.8(2)
O(3)-Cd(1)-O(6)	101.7(2)	O(6)-Cd(1)-O(4)	103.3(2)
O(5)-Cd(1)-O(6)	112.4(2)	O(7)-S(1)-O(8)	114.9(3)
O(3)-Cd(1)-O(4)	112.4(2)		

Bond angle and bond distance of MOF6

Cd-O(4)	2.229(8)	Cd-O(1)#1	2.271(7)
Cd-O(4)#1	2.229(8)	Cd-O(1W)#1	2.365(10)
Cd-O(1)	2.271(7)	Cd-O(1W)	2.365(10)
O(4)-Cd-O(4)#1	180.0	O(1)-Cd-O(1W)#1	88.7(3)
O(4)-Cd-O(1)	93.1(3)	O(1)#1-Cd-O(1W)#1	91.3(3)
O(4)#1-Cd-O(1)	86.9(3)	O(4)-Cd-O(1W)	92.1(3)
O(4)-Cd-O(1)#1	86.9(3)	O(4)#1-Cd-O(1W)	87.9(3)
O(4)#1-Cd-O(1)#1	93.1(3)	O(1)-Cd-O(1W)	91.3(3)
O(1)-Cd-O(1)#1	180.0	O(1)#1-Cd-O(1W)	88.7(3)
O(4)-Cd-O(1W)#1	87.9(3)	O(1W)#1-Cd-O(1W)	180.0(7)
O(4)#1-Cd-O(1W)#1	92.1(3)	Cd-O(1W)-H(1W1)	82(10)
S(1)-O(1)-Cd	137.6(5)	Cd-O(1W)-H(1W2)	128(10)
C(6)-O(4)-Cd	130.4(7)	H(1W1)-O(1W)- H(1W2)	105(5)

Bond angle and bond distance of MOF7

Cd(1)-O(11)	2.218(5)	Cd(2)-O(5)	2.208(5)
Cd(1)-O(13)	2.238(5)	Cd(2)-O(12)	2.248(5)
Cd(1)-O(57)	2.304(5)	Cd(2)-O(2)	2.316(5)
Cd(1)-O(8)	2.321(5)	Cd(2)-O(3)	2.319(5)
Cd(1)-O(58)	2.355(5)	Cd(2)-O(4)	2.368(5)
Cd(1)-O(7)	2.368(4)	Cd(2)-O(1)	2.374(4)
O(2)-Cd(2)-O(3)	117.28(19)	O(11)-Cd(1)-O(7)	135.86(18)
O(5)-Cd(2)-O(4)	100.24(19)	O(13)-Cd(1)-O(7)	84.51(17)
O(12)-Cd(2)-O(4)	84.59(18)	O(57)-Cd(1)-O(7)	92.44(16)
O(2)-Cd(2)-O(4)	171.53(19)	O(8)-Cd(1)-O(7)	55.28(15)
O(3)-Cd(2)-O(4)	54.40(17)	O(58)-Cd(1)-O(7)	123.16(17)
O(5)-Cd(2)-O(1)	136.31(18)	O(5)-Cd(2)-O(12)	104.58(19)
O(12)-Cd(2)-O(1)	84.12(17)	O(5)-Cd(2)-O(2)	81.21(18)
O(2)-Cd(2)-O(1)	55.25(16)	O(12)-Cd(2)-O(2)	103.18(18)
O(3)-Cd(2)-O(1)	92.83(16)	O(5)-Cd(2)-O(3)	112.4(2)
O(4)-Cd(2)-O(1)	123.35(16)	O(12)-Cd(2)-O(3)	127.94(18)
O(57)-Cd(1)-O(8)	115.86(18)	O(11)-Cd(1)-O(13)	104.60(19)
O(11)-Cd(1)-O(58)	100.8(2)	O(11)-Cd(1)-O(57)	111.9(2)
O(13)-Cd(1)-O(58)	85.49(19)	O(13)-Cd(1)-O(57)	129.21(18)
O(57)-Cd(1)-O(58)	54.49(17)	O(11)-Cd(1)-O(8)	80.73(18)
O(8)-Cd(1)-O(58)	170.2(2)	O(13)-Cd(1)-O(8)	103.60(18)
C(32)-O(1)-Cd(2)	91.3(4)	C(32)-O(2)-Cd(2)	92.0(4)
C(27)-O(11)-Cd(1)	129.1(5)	C(53)-O(8)-Cd(1)	92.1(4)
C(21)-O(3)-Cd(2)	92.8(5)	C(21)-O(4)-Cd(2)	90.9(4)
C(17)-O(5)-Cd(2)	129.9(5)	C(53)-O(7)-Cd(1)	91.7(4)
C(115)-O(57)-Cd(1)	92.9(4)	C(115)-O(58)-Cd(1)	91.5(4)

Bond angle and bond distance of MOF8

Cd(1)-O(11)	2.258(10)	Cd(2)-O(10)	2.241(9)
Cd(1)-O(14)	2.249(8)	Cd(2)-O(8)	2.235(10)
Cd(1)-O(18)	2.267(9)	Cd(2)-O(5)	2.274(9)
Cd(1)-O(13)	2.297(10)	Cd(2)-O(22)	2.303(8)
Cd(1)-O(15)	2.317(8)	Cd(2)-O(9)	2.314(9)
Cd(1)-O(12)	2.316(10)	Cd(2)-O(7)	2.325(10)
O(11)-Cd(1)-O(14)	89.7(4)	O(10)-Cd(2)-O(5)	174.5(4)
O(11)-Cd(1)-O(18)	90.0(4)	O(8)-Cd(2)-O(5)	88.6(3)
O(14)-Cd(1)-O(18)	88.9(3)	O(10)-Cd(2)-O(22)	96.9(3)
O(11)-Cd(1)-O(13)	174.7(4)	O(8)-Cd(2)-O(22)	88.6(3)

O(14)-Cd(1)-O(13)	89.4(4)	O(5)-Cd(2)-O(22)	86.2(3)
O(18)-Cd(1)-O(13)	84.8(4)	O(10)-Cd(2)-O(9)	89.7(3)
O(11)-Cd(1)-O(15)	89.8(4)	O(8)-Cd(2)-O(9)	89.4(4)
O(14)-Cd(1)-O(15)	85.1(3)	O(5)-Cd(2)-O(9)	87.3(3)
O(18)-Cd(1)-O(15)	174.0(4)	O(22)-Cd(2)-O(9)	173.2(3)
O(13)-Cd(1)-O(15)	95.2(3)	O(10)-Cd(2)-O(7)	86.4(3)
O(11)-Cd(1)-O(12)	92.8(4)	O(8)-Cd(2)-O(7)	174.0(4)
O(14)-Cd(1)-O(12)	173.6(4)	O(5)-Cd(2)-O(7)	88.8(3)
O(18)-Cd(1)-O(12)	85.1(4)	O(22)-Cd(2)-O(7)	96.7(3)
O(13)-Cd(1)-O(12)	87.6(4)	O(9)-Cd(2)-O(7)	85.0(4)
O(15)-Cd(1)-O(12)	100.8(4)	O(10)-Cd(2)-O(8)	96.0(4)
C(74)-O(5)-Cd(2)	129.4(7)	C(65)-O(14)-Cd(1)	129.6(7)
C(53)-O(7)-Cd(2)	132.7(8)	C(34)-O(12)-Cd(1)	126.8(10)
C(1)-O(8)-Cd(2)	133.9(8)	C(114)-O(10)-Cd(2)	122.4(8)
C(28)-O(13)-Cd(1)	132.1(8)	C(113)-O(9)-Cd(2)	120.1(8)
C(24)-O(11)-Cd(1)	132.3(9)		

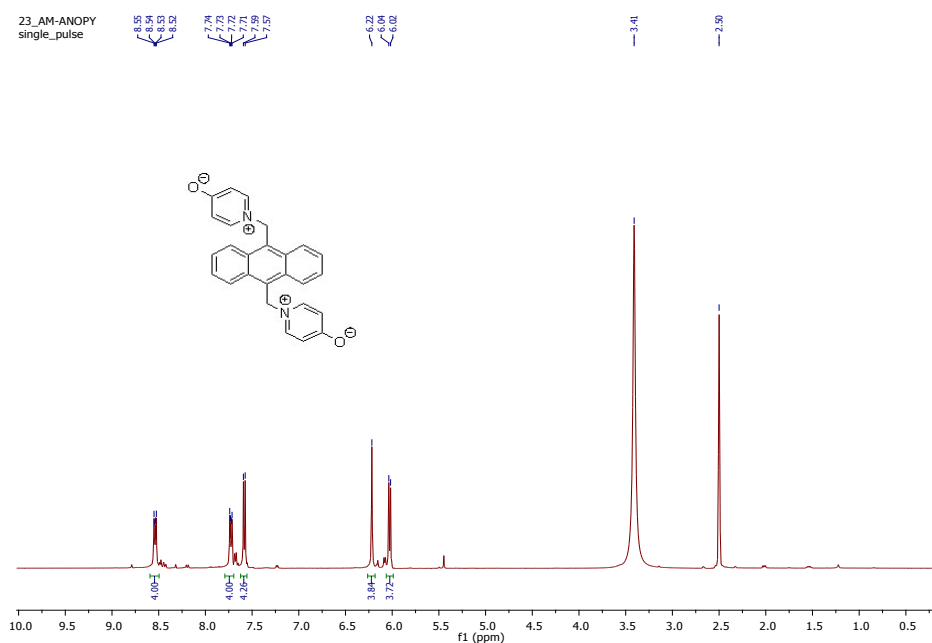


Figure S1. ^1H -NMR spectrum of 1,1'-(anthracene-9,10-diylbis(methylene))bis(pyridin-1-ium-4-olate) (AHP).

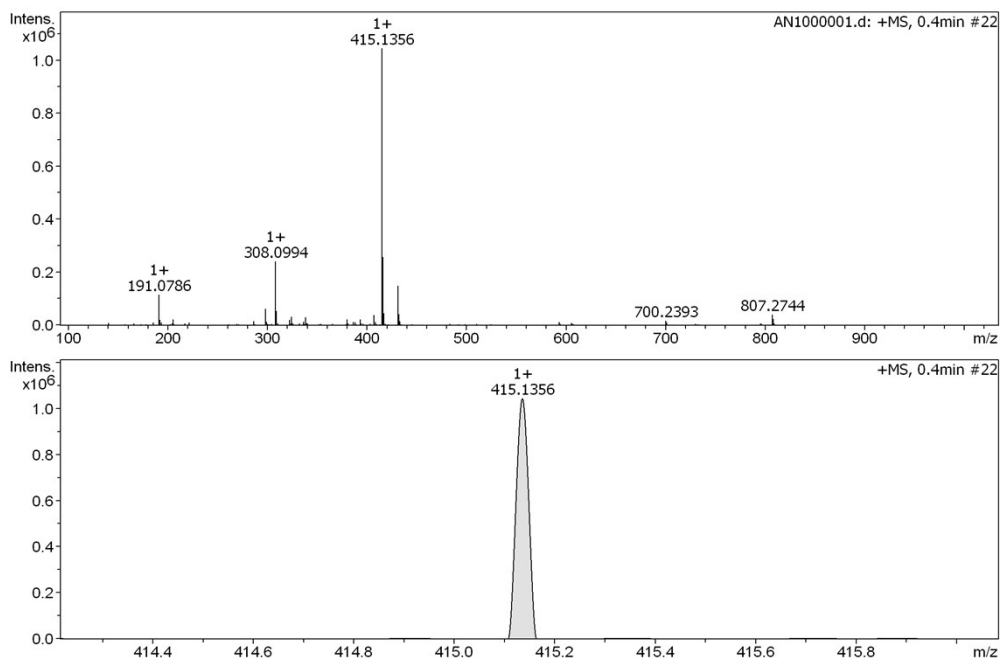


Figure S2. ESI-MS spectrum of 1,1'-(anthracene-9,10-diylbis(methylene))bis(pyridin-1-ium-4-olate) (AHP).

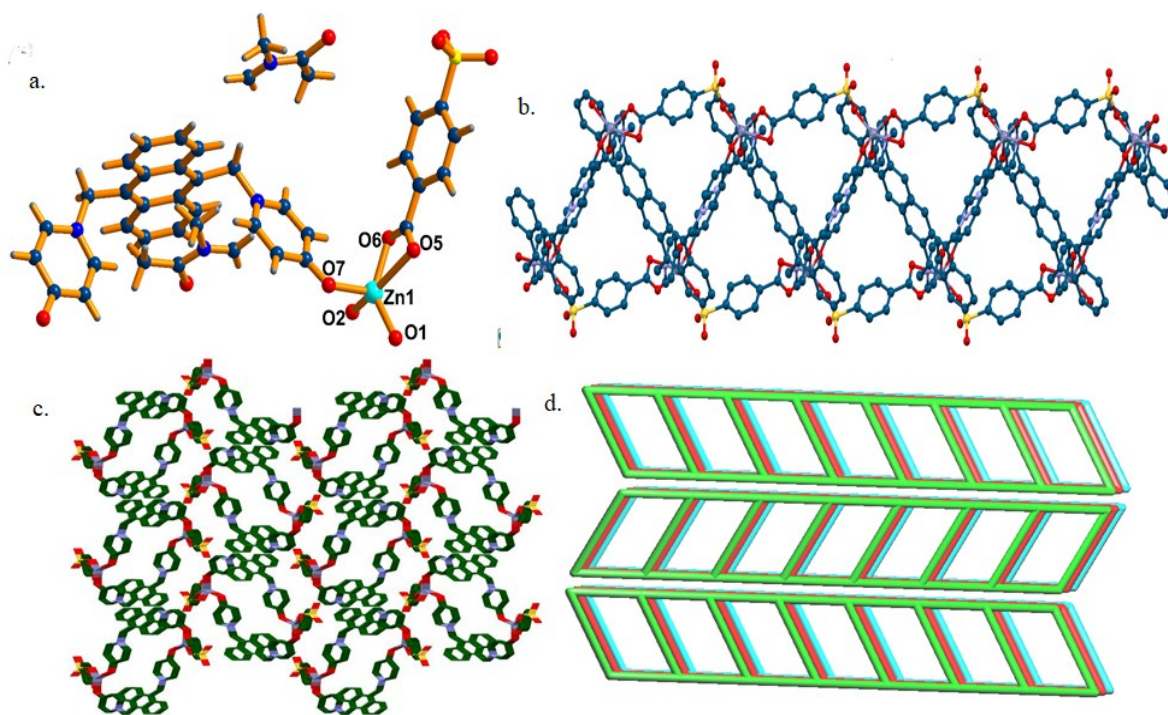


Figure S3. a. Crystal structure of MOF2, b. 2D sheet in ac-plane formed by bridging 4-SBA, c. 2D network of MOF2 stabilized by $\pi \dots \pi$ interaction, d. Topological representation of MOF2.

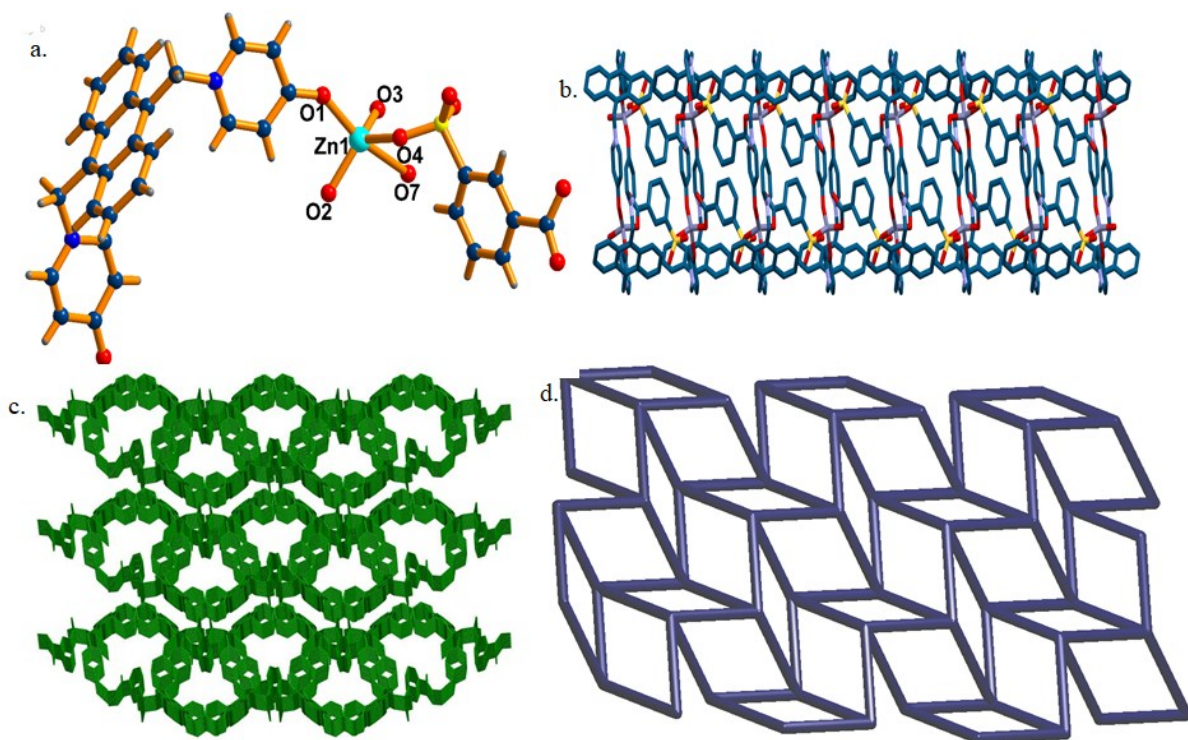


Figure S4. a. Crystal structure of MOF3, b. View of the 2D framework built from 1D corrugated chains and 3-SBA ligands along a axis, c. 3D network, d. Topological representation of MOF3.

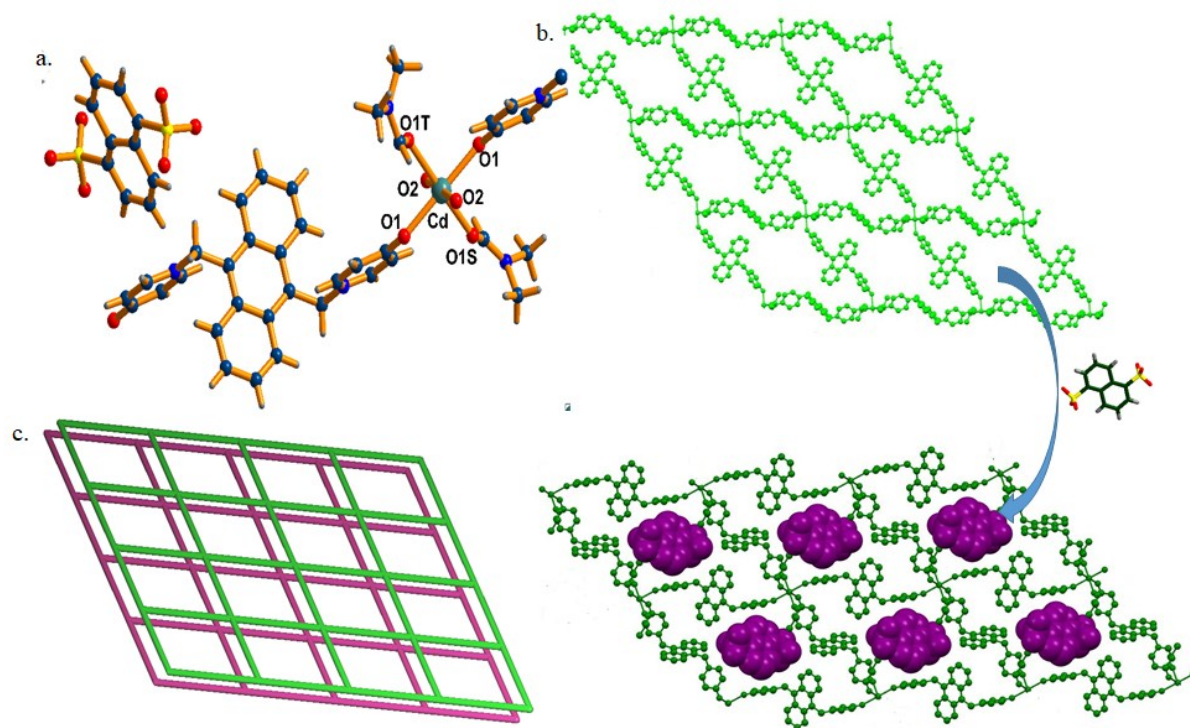


Figure S5. a. Crystal structure of MOF4, b. Host-guest assembly, c. Topological representation of MOF4.

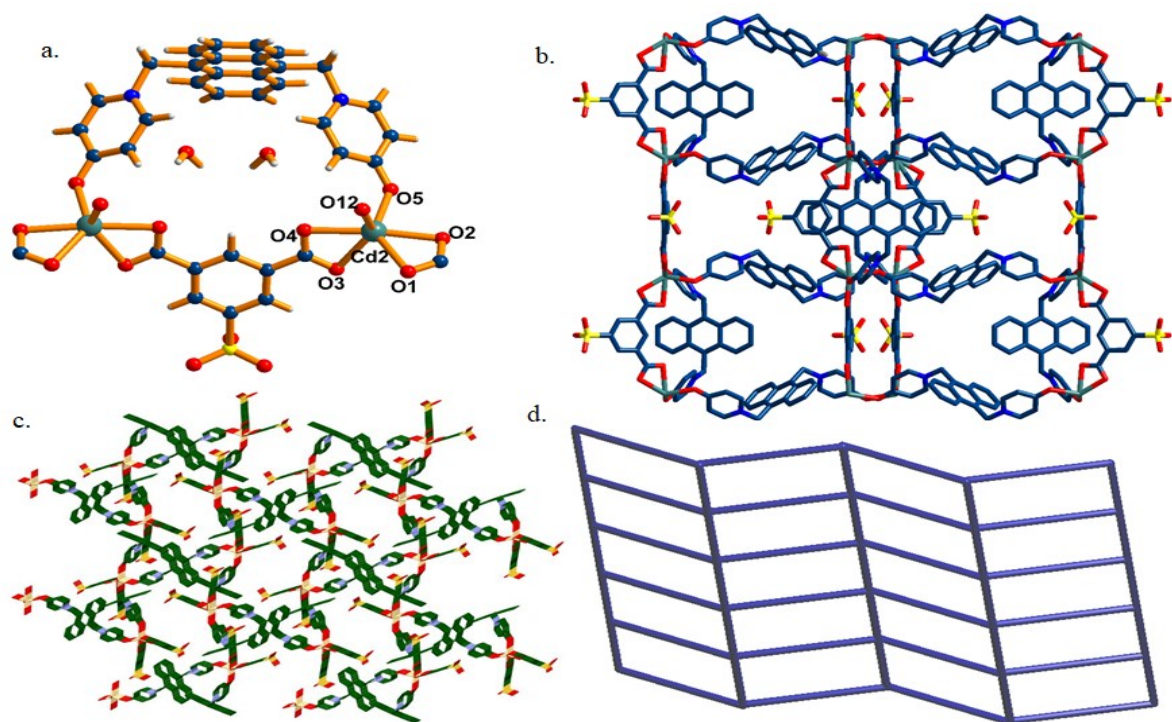


Figure S6. a. Crystal structure of MOF7, b. 2D framework along b axis, c. Formation of 3D network through O-H...O interactions, d. Topological representation of MOF7.

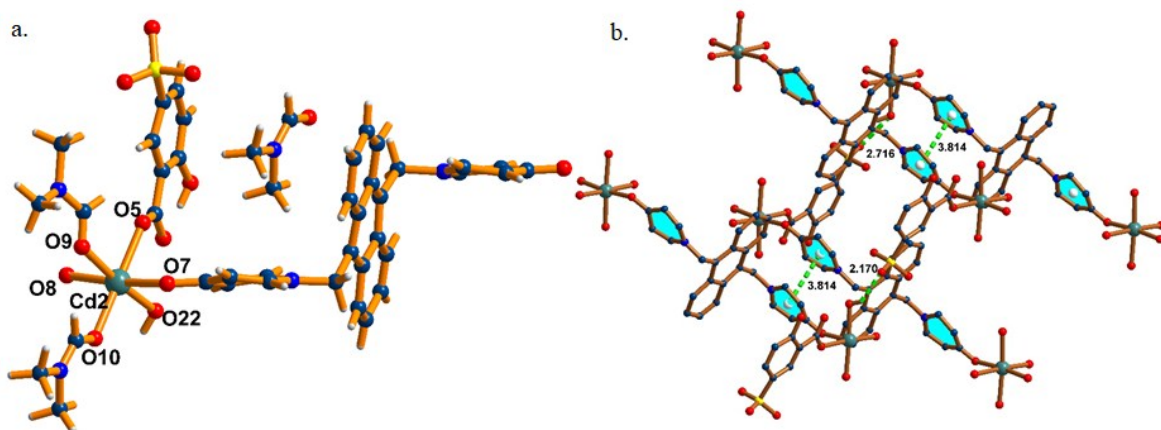


Figure S7. a. Crystal structure of MOF8, b. C-H...O and π - π interactions in MOF8.

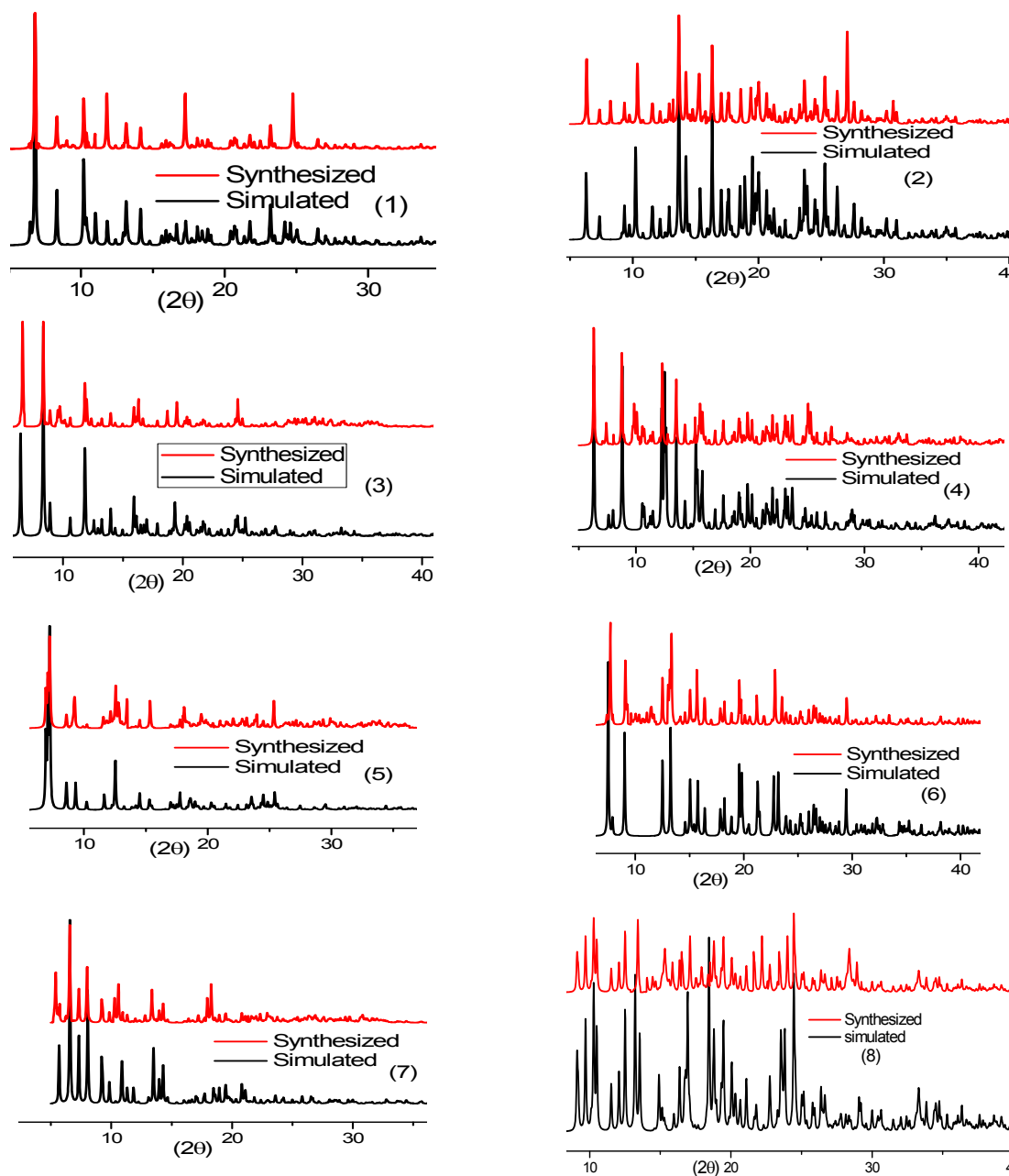


Figure S8. Powder X-ray diffraction patterns of MOF1-8 [synthesized (red) and simulated (black)].

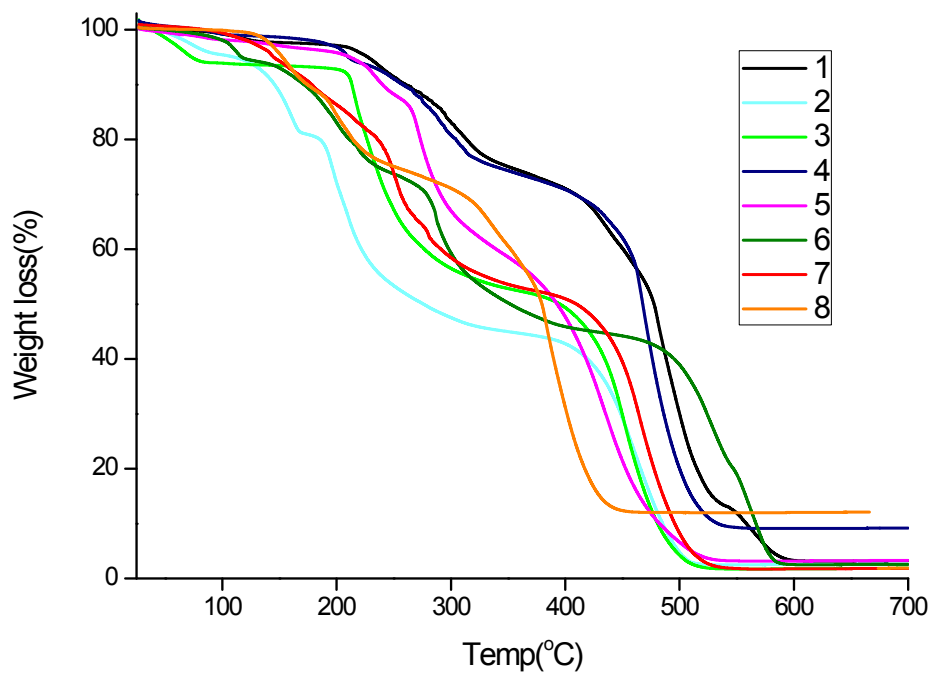


Figure S9. The TG curves for MOFs1-8.

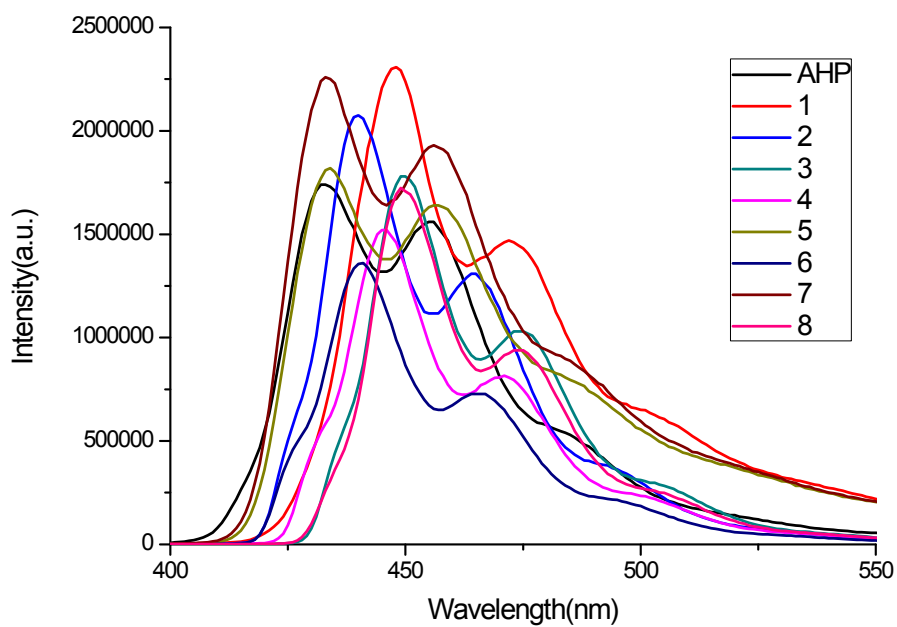


Figure S10. Emission spectra of AHP and MOFs1-8.

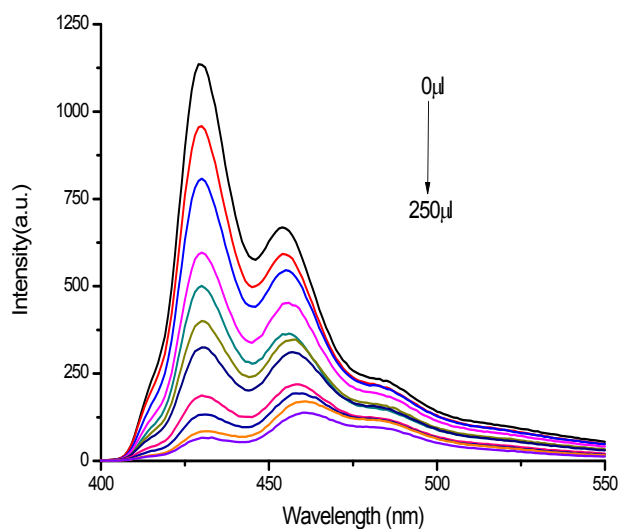


Figure S11a. Fluorescence sensing of trinitrophenol (PA) by MOF5 in DMF.

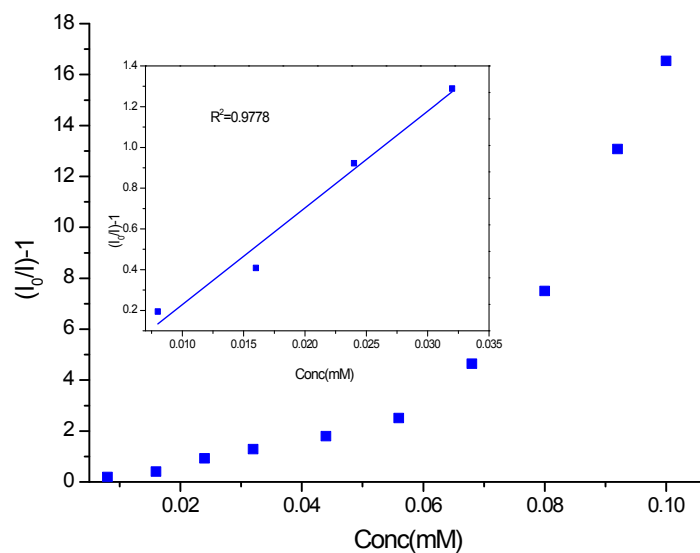


Figure S11b. Stern-Volmer plot for the fluorescence quenching of MOF5 upon addition of PA. Inset: The Stern-Volmer plot at low PA concentrations.

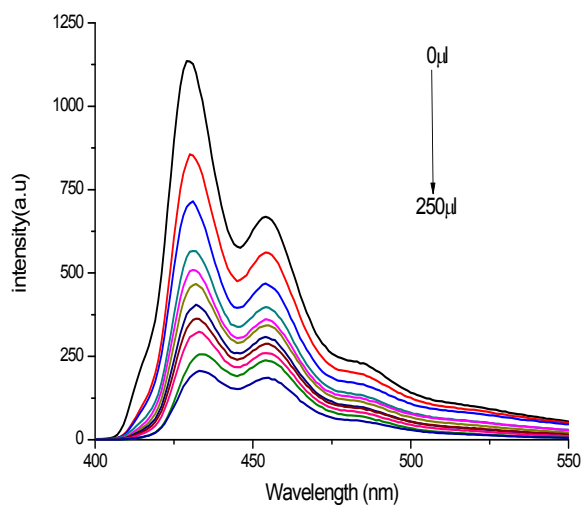


Figure S12a. Fluorescence sensing of dinitrophenol (DNP) by MOF5 in DMF.

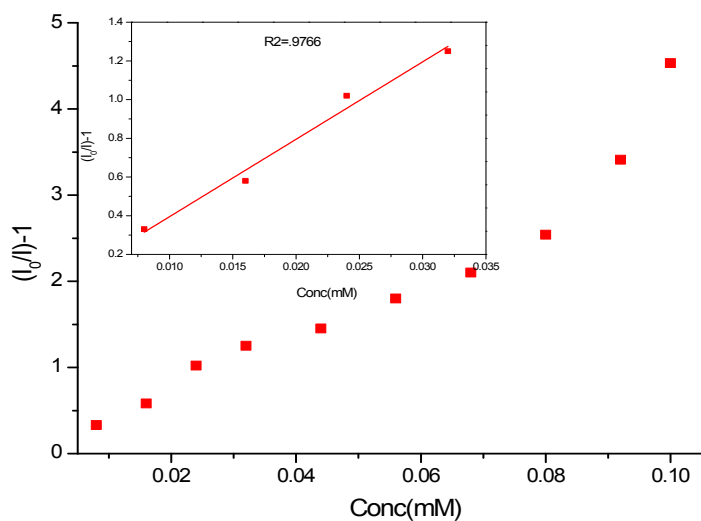


Figure S12b. Stern-Volmer plot for the fluorescence quenching of MOF5 upon addition of DNP. Inset: The Stern-Volmer plot at low DNP concentrations.

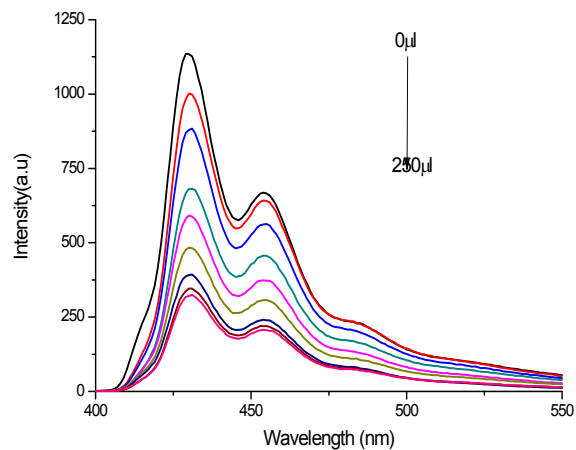


Figure S13a. Fluorescence sensing of nitrophenol (NP) by MOF5 in DMF.

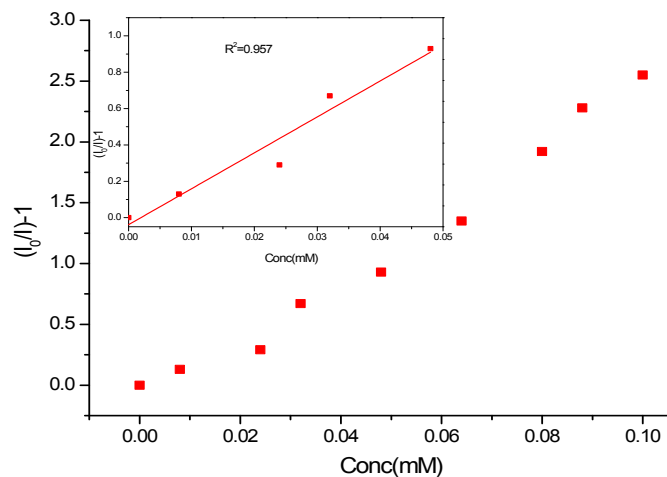


Figure S13b. Stern-Volmer plot for the fluorescence quenching of MOF5 upon addition of NP. Inset: The Stern-Volmer plot at low NP concentrations.

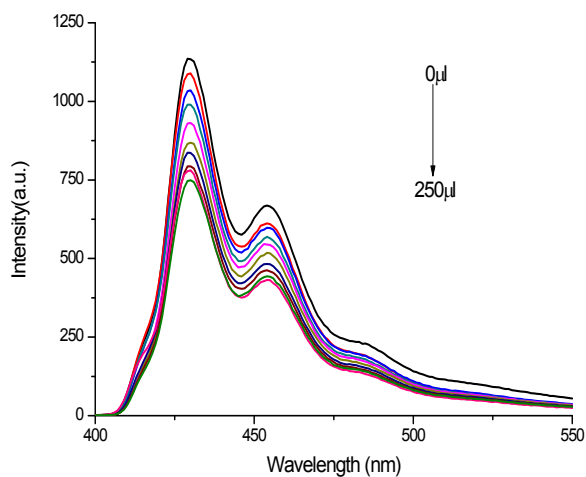


Figure S14a. Fluorescence sensing of simazine by MOF5 in DMF.

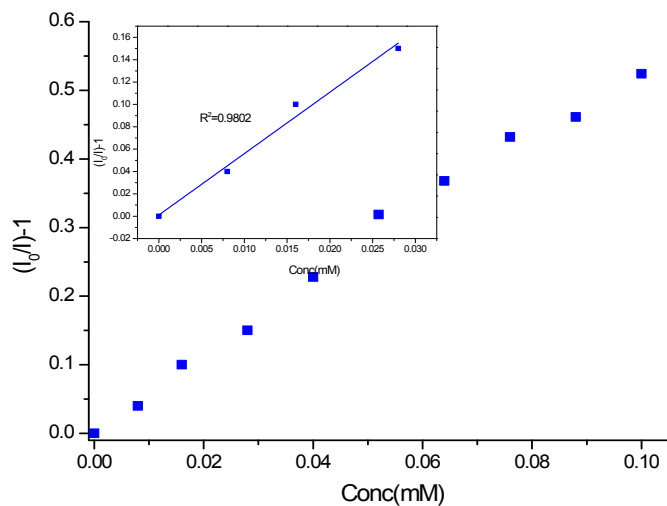


Figure S14b. Stern-Volmer plot for the fluorescence quenching of MOF5 upon addition of simazine. Inset: The Stern-Volmer plot at low simazine concentrations.

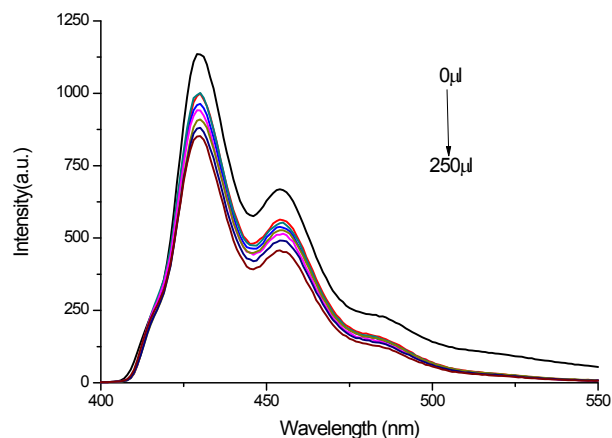


Figure S15a. Fluorescence sensing of NT (nitrotoluene) by MOF5 in DMF.

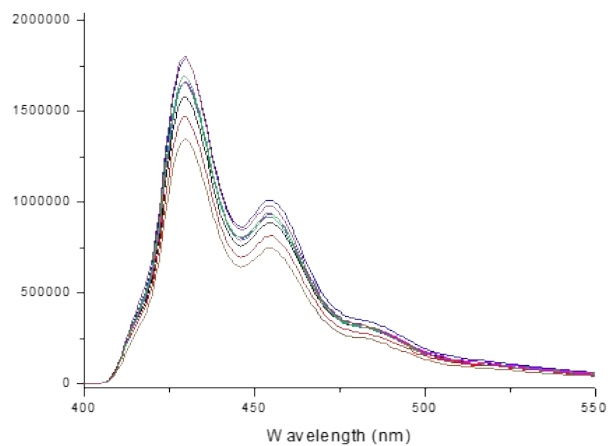


Figure S15b. Fluorescence sensing of 4-methoxy phenol by MOF7 in DMF.

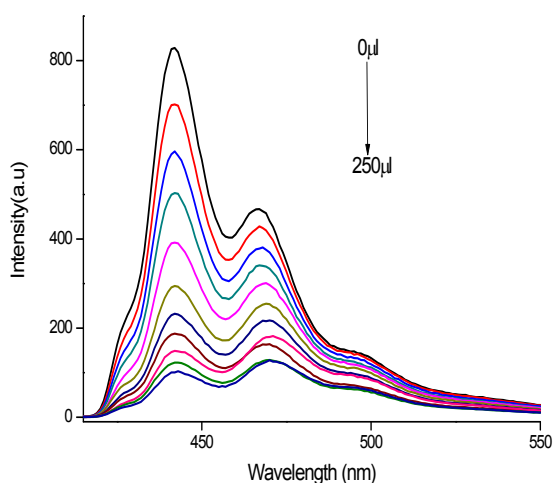


Figure S16a. Fluorescence sensing of trinitrophenol (PA) by MOF6 in DMF.

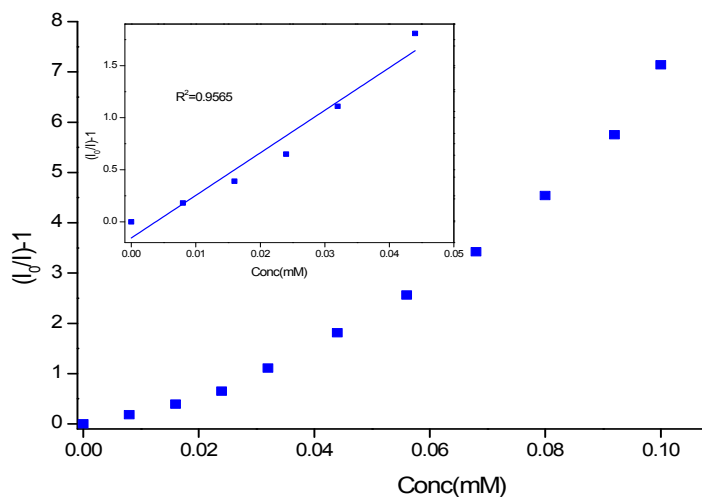


Figure S16b. Stern–Volmer plot for the fluorescence quenching of MOF6 upon addition of PA. Inset: The Stern–Volmer plot at low PA concentrations.

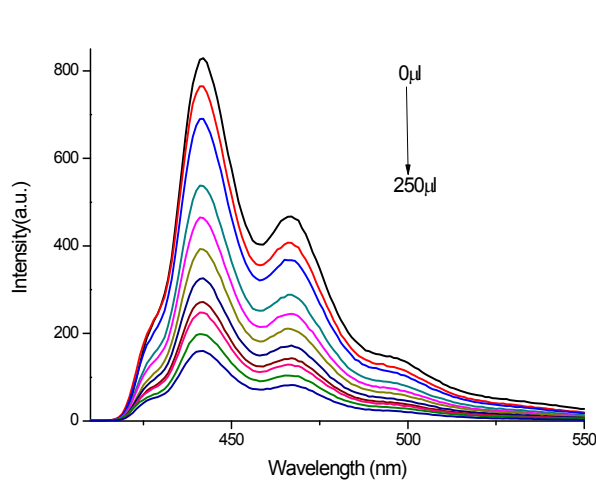


Figure S17a. Fluorescence sensing of nitrophenol (DNP) by MOF6 in DMF.

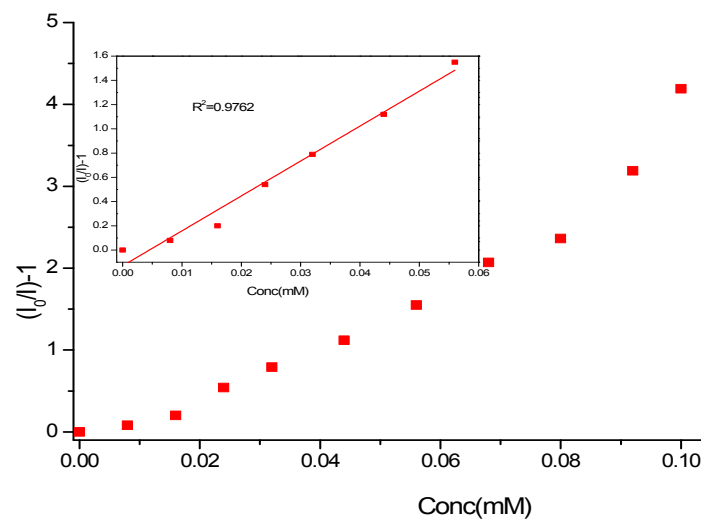


Figure S17b. Stern-Volmer plot for the fluorescence quenching of MOF6 upon addition of DNP. Inset: The Stern-Volmer plot at low DNP concentrations.

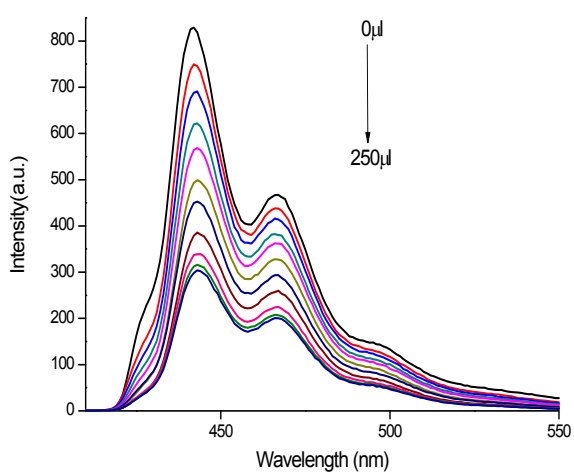


Figure S18a. Fluorescence sensing of nitrophenol (NP) by MOF6 in DMF.

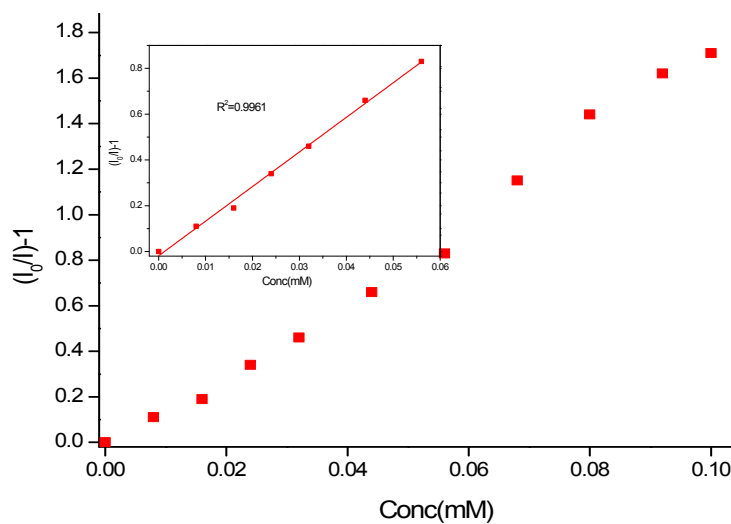


Figure S18b. Stern-Volmer plot for the fluorescence quenching of MOF6 upon addition of NP. Inset: The Stern-Volmer plot at low NP concentrations.

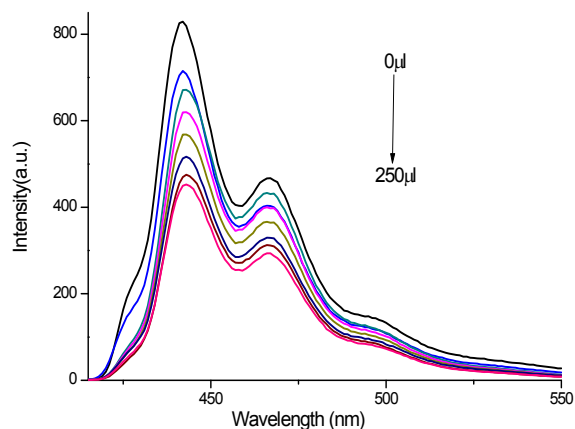


Figure S19a. Fluorescence sensing of simazine by MOF6 in DMF.

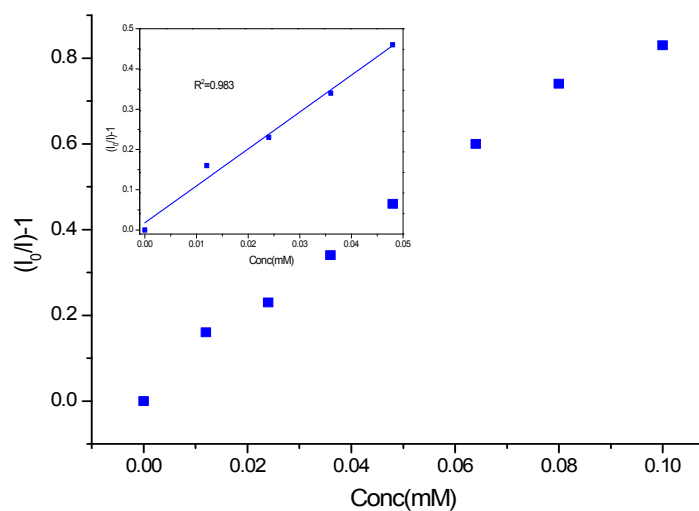


Figure S19b. Stern–Volmer plot for the fluorescence quenching of MOF6 upon addition of simazine. Inset: The Stern–Volmer plot at low simazine concentrations.

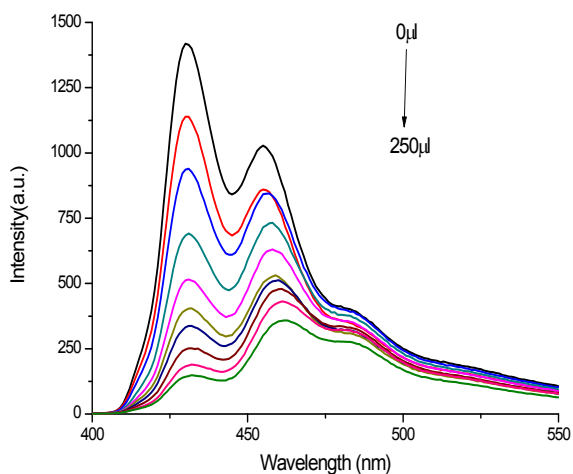


Figure S20a. Fluorescence sensing of trinitrophenol (PA) by MOF7 in DMF.

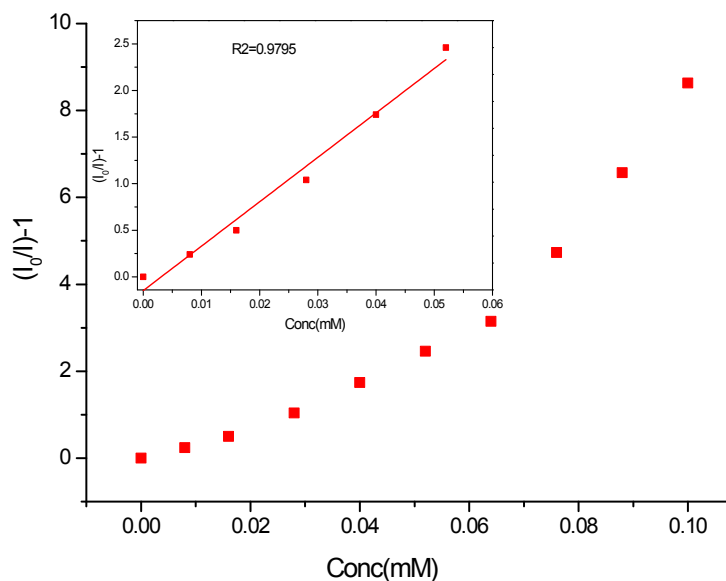


Figure S20b. Stern–Volmer plot for the fluorescence quenching of MOF7 upon addition of PA. Inset: The Stern–Volmer plot at low PA concentrations.

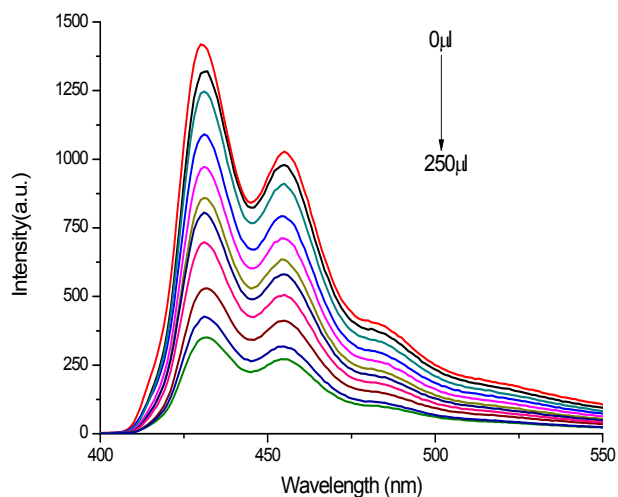


Figure S21a. Fluorescence sensing of dinitrophenol (DNP) by MOF7 in DMF.

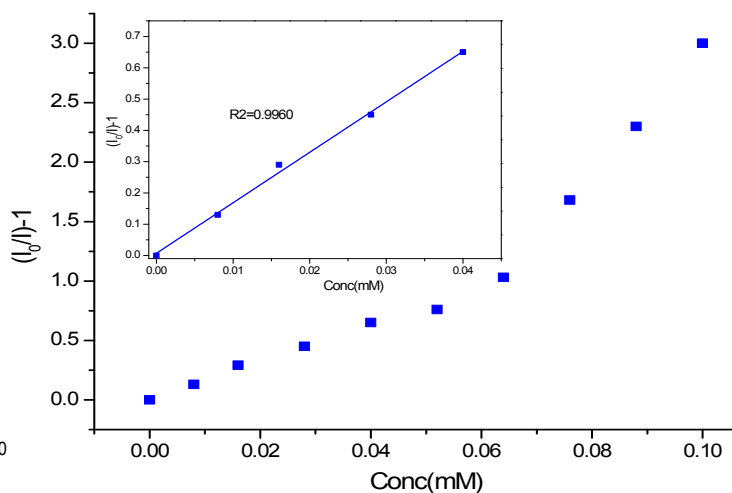


Figure S21b. Stern–Volmer plot for the fluorescence quenching of MOF7 upon addition of DNP. Inset: The Stern–Volmer plot at low DNP concentrations.

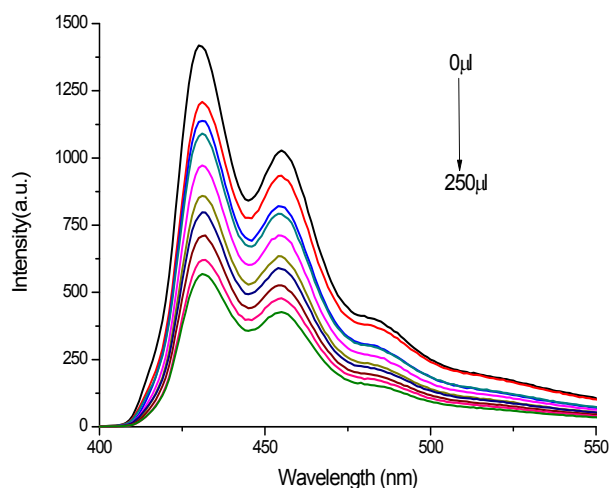


Figure S22a. Fluorescence sensing of nitrophenol (NP) by MOF7 in DMF.

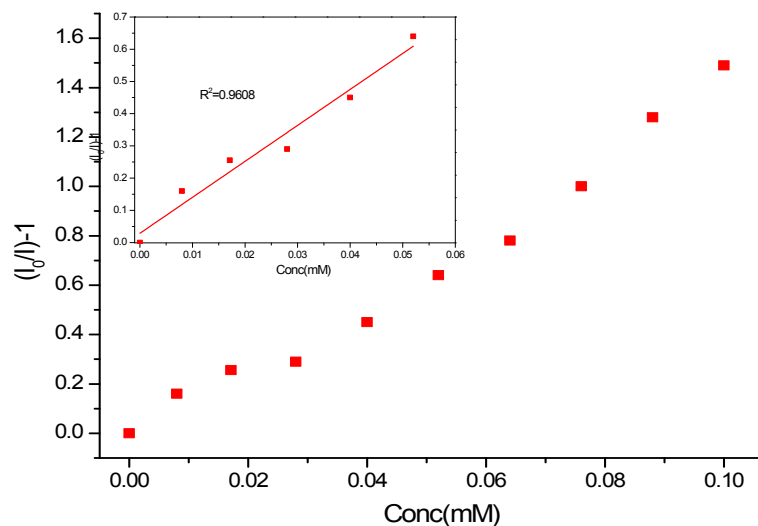


Figure S22b. Stern–Volmer plot for the fluorescence quenching of MOF7 upon addition of NP. Inset: The Stern–Volmer plot at low NP concentrations.

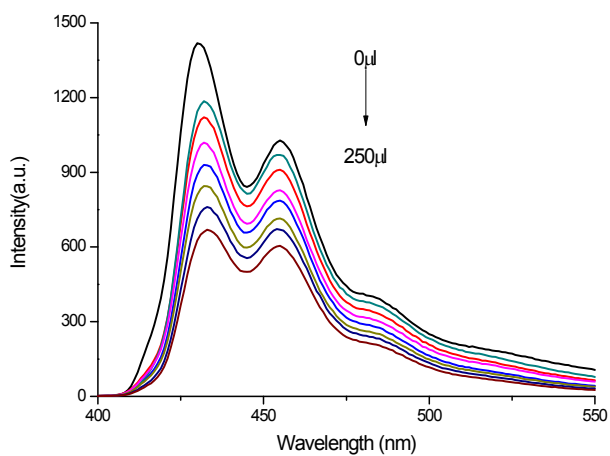


Figure S23a. Fluorescence sensing of simazine by MOF7 in DMF.

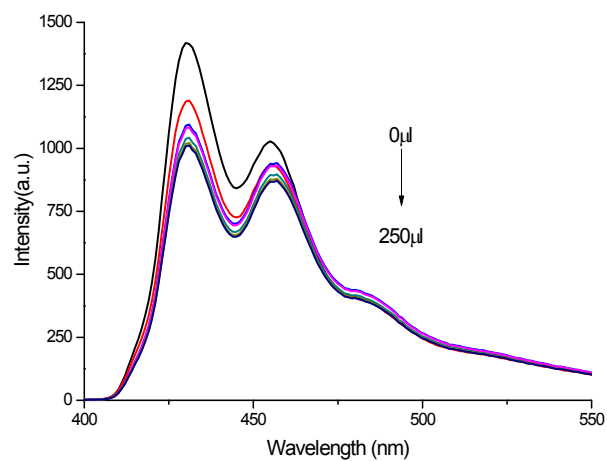


Figure S23b. Fluorescence sensing of NT (nitrotoluene) by MOF7 in DMF.

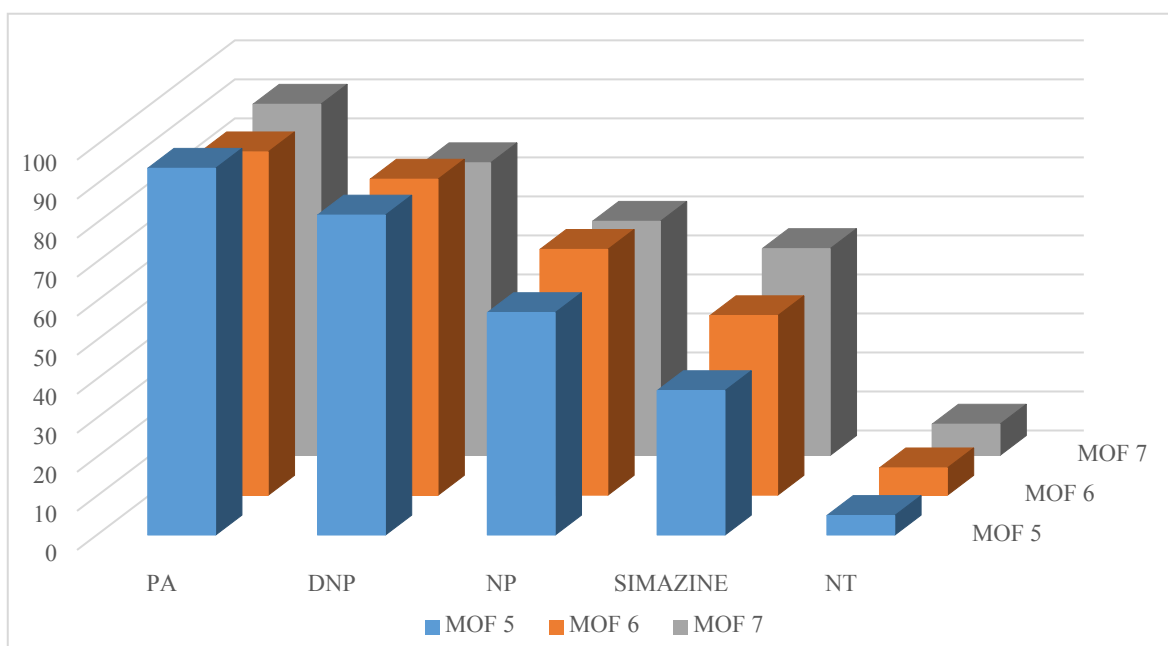


Figure S24. The fluorescence quenching efficiencies of different MOFs5-7.

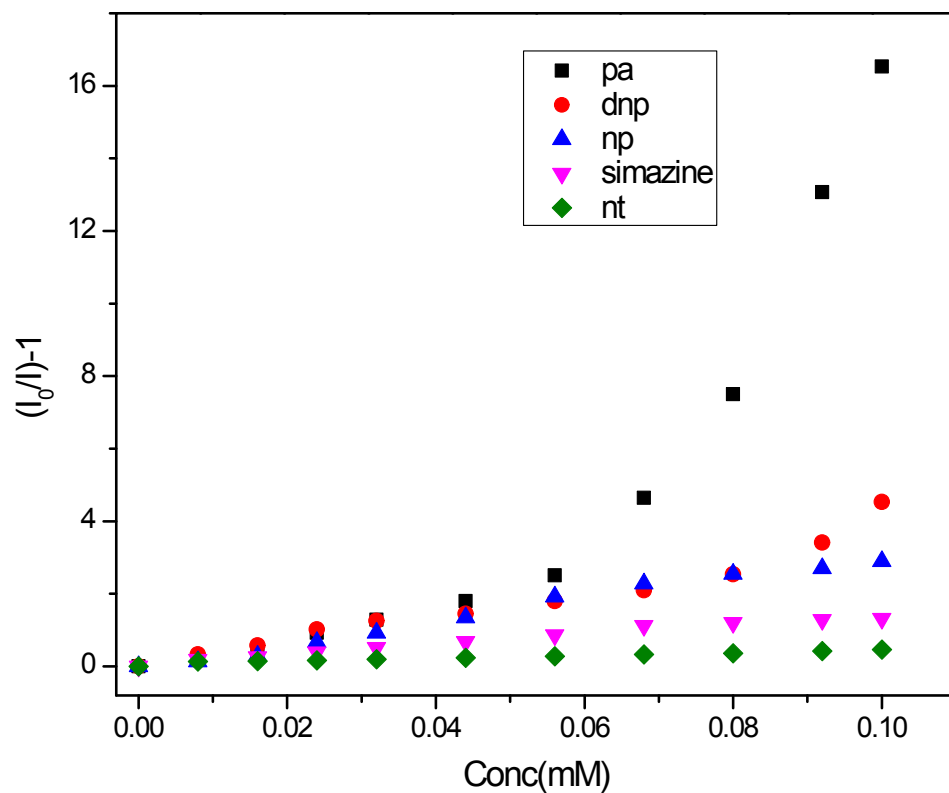


Figure S25. Stern–Volmer plots for MOF5 upon gradual addition of NACs and simazine.

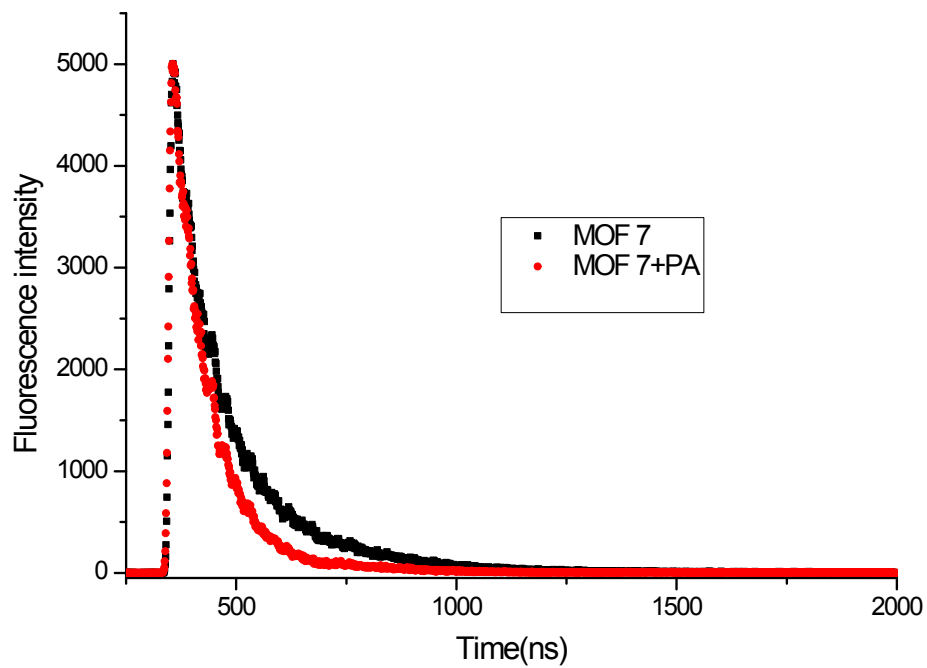


Figure S26. Fluorescence decay profile of MOF7 in the presence and absence of PA.

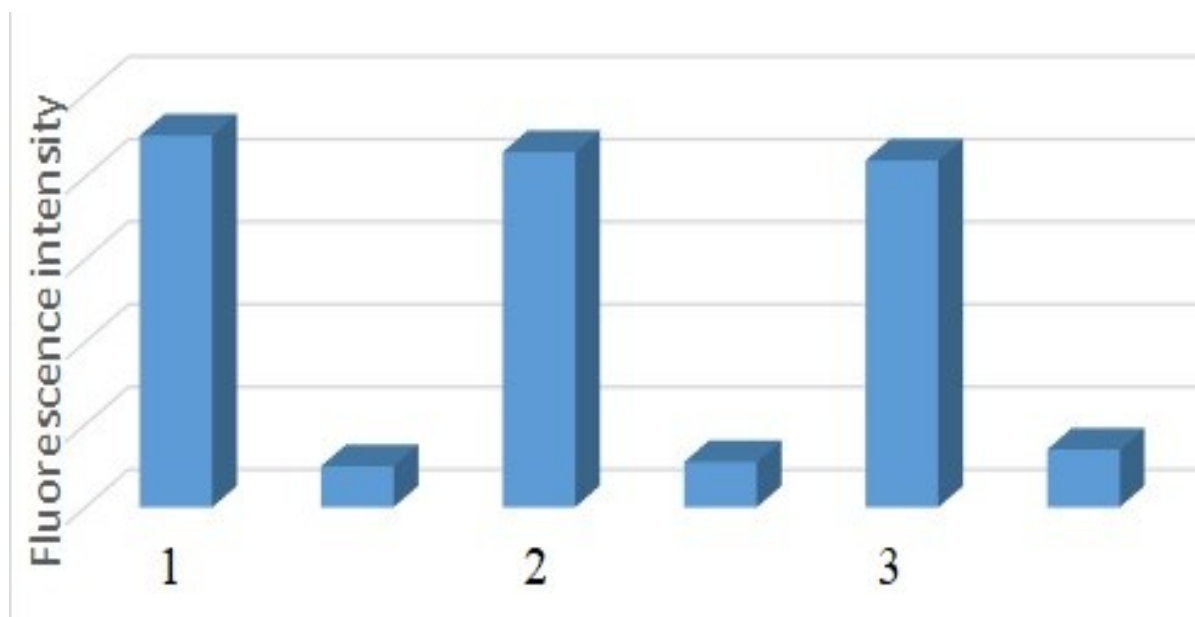


Figure S27. Recyclability test of MOF7 represent the fluorescence intensities of MOF7 before and after the addition of PA in each cycle

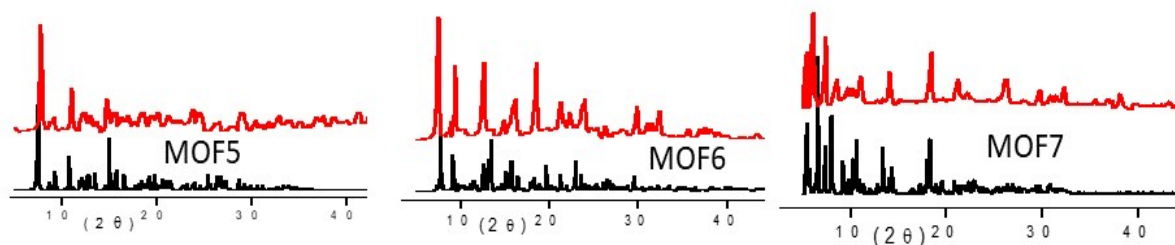


Figure S28. Powder XRD patterns of MOFs5-7 before (black) after treatment (red) with PA

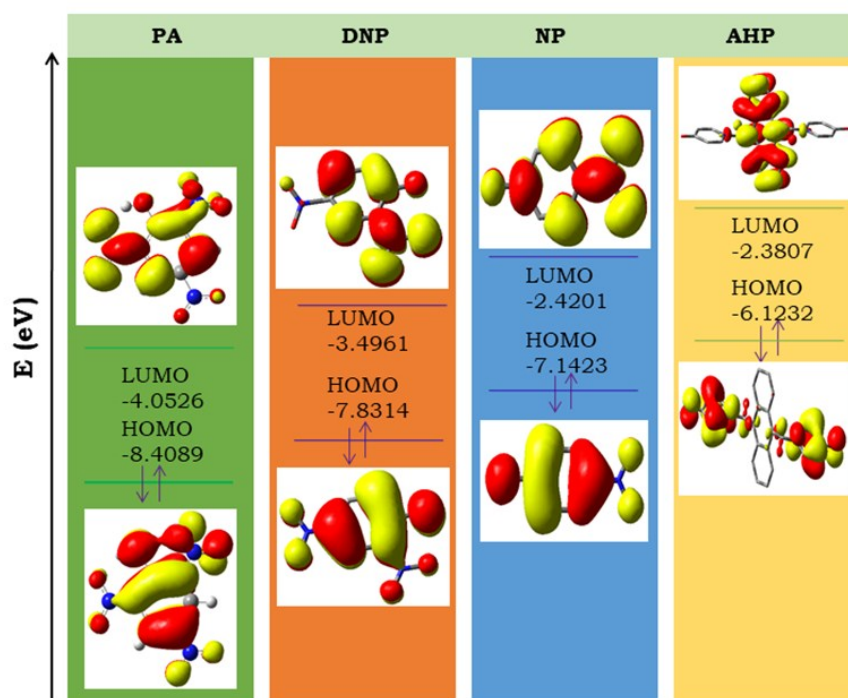


Figure S29. Comparison of HOMO and LUMO energies of PA, DNP, NP and AHP.

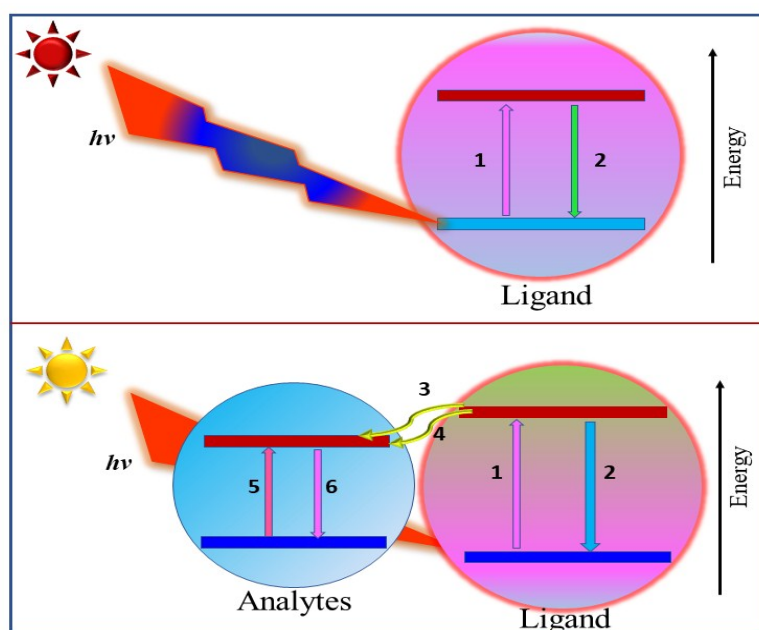


Figure S30. Schematic representation of various energy/electron transfer processes in the absence and presence of analytes. 1. Excited ligand center, 2. Ligand based luminescence, 3. Energy transfer from ligand to analyte, 4. Electron transfer from ligand to analytes, 5. Absorption of light by the analytes, 6. Analytes based luminescence.

Table S3. Reported size of nano MOFs

NMOF	Size	Ref.
MIL-100	200 nm	6
Fe ₃ (μ ₃ -O)Cl(H ₂ O)(BDC) ₃	<200nm	7
Mn-IR-825	40 nm	8
ZIF-8	90 +- 15	9
Mn-IR825@PDA-PEG	70nm	10
nMOF-253	50 nm	11
TBC-Hf,	50-100 nm	12
PCN-224	90 nm	13

Table S4. Quenching Constants (K_{SV}) for the PA, DNP, NP and Simazine

NACs	MOF5	MOF6	MOF7
PA	4.5×10 ⁴	4.0×10 ⁴	5.0×10 ⁴
DNP	3.9×10 ⁴	2.8×10 ⁴	1.6×10 ⁴
NP	1.9×10 ⁴	1.5×10 ⁴	1.5×10 ⁴
Simazine	5.6×10 ³	9.1×10 ³	9.4×10 ³

Table S5. Standard deviation and detection limit calculation for NP, DNP, PA and Simazine

	MOF5	MOF6	MOF7
1	1140.152	831.059	1416.353
2	1141.298	830.851	1415.128
3	1139.034	832.048	1417.323
4	1141.363	831.917	1415.018
5	1140.897	830.218	1416.895

Standard deviation(σ)	0.871497	0.683735	0.92713
LOD (NP)	13.7×10^{-5}	13.6×10^{-5}	1.85×10^{-4}
LOD (DNP)	6.70×10^{-5}	7.32×10^{-5}	1.73×10^{-4}
LOD (PA)	5.81×10^{-5}	5.10×10^{-5}	5.5×10^{-5}
LOD (simazine)	4.66×10^{-4}	2.25×10^{-4}	2.95×10^{-4}

Table S6. A comparison of the Stern-Volmer constant (Ksv), detection limit with other MOFs.

		Quenching constant (M^{-1})	Limit of Detection (LOD)	Ref.
	Cd.AHP.1,5-NDS	4.52×10^4	5.81×10^{-5}	Present
	Cd.AHP.2,6-NDS.DMF.2H ₂ O	4.11×10^4	5.10×10^{-5}	work
	Cd.AHP.SIA.2H ₂ O	5.01×10^4	5.5×10^{-5}	
1	$[(CH_3)_2NH_2]_3[Zn_4Na(BPTC)_3] \cdot 4CH_3OH \cdot 2DMF$	3.2×10^4	5 μ M	14
2	$\{[Zn(IPA)(L_{14})]\}_n$ $\{[Cd(IPA)(L_{14})]\}_n$	1.16×10^4 1.35×10^4	(0.12 μ M) (0.06 μ M)	15
3	Zr ₆ O ₄ (OH) ₄ (L ₂) ₆	2.9×10^4	2.6 μ M	16
4	BUT-13	5.1×10^5	4.9×10^{-7}	17
5	SNNU-110	2.3×10^4	1.94 ppm	18
6	$[NH_2(CH_3)_2][Zn_4O-(bpt)_2(bdc)_{0.5}] \cdot 5DMF$	1.69×10^4	1.87×10^{-7}	19
7	$[Zn(L)(dipb)](H_2O)_2$	2.46×10^4	-	20
8	$[Zn_8(ad)_4(BPDC)6O \cdot 2Me_2NH_2] \cdot G$; (G = DMF and Water)	4.6×10^4	4×10^{-8}	21
9	Dy-MOF (1)	8.55×10^4	1×10^{-6} M	22
10	(DMF) _x (H ₂ O) _y @[In(OH)(H ₂ DOBDC)]	8.33×10^4	66 \pm 8 ppb	23

11	Tb-MDIA	6.3×10^4	$5 \times 10^{-7}\text{M}$	24
12	USTC-7	4.90×10^4	$2.78 \times 10^{-4}\text{mM}$	25
13	$\{\text{Cd}(\text{INA})(\text{pytpy})(\text{OH}) \cdot 2\text{H}_2\text{O}\}_n$	4.3×10^4	2.41×10^{-6}	26
14	$[\text{Cd}_4(\text{L})_2(\text{L}_2)_3(\text{H}_2\text{O})_2]$	3.89×10^4	1.98 ppm	27
15	$[\text{Cd}_2(\text{Lws})(\text{OH})]_n$	2.23×10^4	1.12×10^{-5}	28
16	$[\text{Zn}_2(\text{TPOM})(\text{NH}_2\text{-BDC})_2] \cdot 4\text{H}_2\text{O}$	4.6×10^4	9.8×10^{-7}	29
17	$[\text{Cd}_5\text{Cl}_6(\text{L})(\text{HL})_2] \cdot 7\text{H}_2\text{O}$	4.05×10^4	1.87×10^{-7}	30
18	$\text{Zn}_2(\text{TZBPDC})(\mu_3\text{-OH})(\text{H}_2\text{O})_2$	4.9×10^4	2.87×10^{-7}	31
19	Cd-CP	13.9×10^4	0.054 (12.4 \pm 0.1 ppb)	32
20	In-ADBA	1.282×10^5	-	33
21	$[\text{Zn}_4(\text{DMF})(\text{Ur})_2(2,6\text{-NDC})_4]_n$	10.83×10^4	1.63 ppm	34

References

- 1 G M. Sheldrick. SADABS, University of Göttingen, Germany, 1996.
- 2 G. M. Sheldrick. *Acta Crystallogr., Sect. A: Found. Crystallogr.*, 1990, **46**, 467–473.
- 3 G. M. Sheldrick. SHELXTL-NT 2000 version 6.12, reference manual, University of Göttingen, Göttingen, Germany.
- 4 K. Brandenburg, Diamond: visual crystal structure information system (Version 2.1d), crystal impact GbR, Bonn, Germany, 2000.
- 5 Mercury, Cambridge Crystallographic Data Centre, 12 Union Road, Cambridge CB2 1EZ, United Kingdom. Available from: Website: <http://www.ccdc.cam.ac.uk/>.
- 6 P. Horcajada, T. Chalati, C. Serre, B. Gillet, C. Sebrie, T. Baati and J. S. Chang, *Nat. mat.*, 2010, **9**, 172-178.

- 7 K. M. Taylor-Pashow, J. Della Rocca, Z. Xie, S. Tran and W. Lin, *J. Am. Chem. Soc.*, 2009, **131**, 14261-14263.
- 8 Y. Yang, J. Liu, C. Liang, L. Feng, T. Fu, Z. Dong, Y. Chao, Y. Li, G. Lu, M. Chen and Z. Liu, *ACS Nano*, 2016, **10**, 2774-2781.
- 9 C. Tamames-Tabar, D. Cunha, E. Imbuluzqueta, F. Ragon, C. Serre, M. J. Blanco-Prieto and P. Horcajada, *J. Mater. Chem. B*, 2014, **2**, 262-271.
- 10 L. Wang, M. Zheng, and Z. Xie, *J. Mater. Chem., B*, 2018, **6**, 707-717.
- 11 Y. Lu, B. Yan and J. L. Liu, *Chem. Commun.*, 2014, **50**, 9969-9972.
- 12 K. Lu, C. He, N. Guo, C. Chan, K. Ni, R. R. Weichselbaum and W. Lin, *J. Am. Chem. Soc.*, 2016, **138**, 12502–12510.
- 13 J. Park, Q. Jiang, D. Feng, L. Mao and H. C. Zhou, *J. Am. Chem. Soc.*, 2016, **138**, 3518–3525.
- 14 E. L. Zhou, P. Huang, C. Qin, K. Z. Shao and Z. M. Su, *J. Mater. Chem., A*, 2015, **3**, 7224-7228.
- 15 B. Parmar, Y. Rachuri, K. Bisht, K. Laiya and R. E. Suresh, *Inorg. Chem.*, 2017, **56**, 2627-2638.
- 16 S. S. Nagarkar, V. A. Desai and S. K. Ghosh, *Chem. Commun.*, 2014, **50**, 8915-8918.
- 17 W. Bin, L. Xiu-Liang, F. Dawei, X. Lin-Hua, Z. Jian, L. Ming, X. Yabo, L. Jian-Rong and H. Caiz, *J. Am. Chem. Soc.*, 2016, **138**, 6204-6216.
- 18 H. P. Li, Z. Dou, S. Q. Chen, M. Hu, S. Li, H. M. Sunand and Q. G. Zhai, *Inorg. Chem.*, 2019, **58**, 11220-11230.
- 19 S. Xing, Q. Bing, H. Qi, J. Liu, T. Bai, G. Li, Z. Shi, S. Feng and R. Xu, *ACS Appl. Mater. Interfaces*, 2017, **9**, 23828-23835.
- 20 Z. Q. Shi, Z. J. Guo and H. G. Zheng, *Chem. Commun.*, 2015, **51**, 8300-8303.
- 21 B. Joarder, A. V. Desai, P. Samanta, S. Mukherjee and S. K. Ghosh, *Chem. Eur. J.* 2014, **20**, 1-6.
- 22 R. Rajak, M. Saraf, S. K. Verma, R. Kumar and S. M. Mobin, *Inorg. Chem.*, 2019, **58**, 16065-16074.
- 23 A. Sharma, D. Kim, J.-H. Park, S. Rakshit, J. Seong, G. H. Jeong, O.-H. Kwon and M. S. Lah, *Commun. Chem.*, 2019, **2**, 1-8.
- 24 P. Wu, L. Xia, M. Huangfu, F. Fu, M. Wang, B. Wen and J. Wang, *Inorg. Chem.*, 2020, **59**, 264-273.
- 25 Y. L. Hu, M. L. Ding, X. Q. Liu, L. B. Sun and H. L. Jiang, *Chem. Commun.*, 2016, **52**, 5734–5737.

- 26 J. Zhang, J. Wu, G. Tang, J. Feng, F. Luo, B. Xu and C. Zhang, *Sens. Actuators B: Chem.*, 2018, **272** 166–174.
- 27 T. K. Pal, N. Chatterjee and P. K. Bharadwaj, *Inorg. Chem.*, 2016, **55**, 1741-1747.
- 28 X. F. Yang, H. B. Zhu and M. Liu, *Polyhedron*, 2017, **128** 18–29.
- 29 R. Lv, J.Y. Wang, Y.P. Zhang, H. Li, L.Y. Yang, S.Y. Liao, W. Gu and X. Liu, *J. Mater. Chem., A* 2016, **4**, 15494–15500.
- 30 A. Buragohain, M. Yousufuddin, M. Sarma and S. Biswas, *Cryst. Growth Des.*, 2016, **16**, 842–851.
- 31 Y. L. Hu, M. L. Ding, X. Q. Liu, S. L. Bing and H. L. Jiang, *Chem. Commun.*, 2016, **52**, 5734–5737.
- 32 S. I. Vasylevskiy, D. M. Bassani and K. M. Fromm, *Inorg. Chem.*, 2019, **58**, 5646–5653.
- 33 X. Liu, B. Liu, G. Li and Y. Liu, *J. Mater. Chem., A*, 2018, **6**, 17177–17185.
- 34 S. Mukherjee, A. V. Desai, B. Manna, A. I. Inamdar and S. K. Ghosh, *Cryst. Growth Des.*, 2015, **15**, 4627–4634.